AFRL-RD-PS-
JA-2015-0001

AFRL-RD-PS-
JA-2015-0001

ALL CAVITY-MAGNETRON AXIAL EXTRACTION TECHNIQUE (POSTPRINT)

Brad W. Hoff, et al.

11 November 2012

Journal Article

AIR FORCE RESEARCH LABORATORY
Directed Energy Directorate
3550 Aberdeen Ave SE
AIR FORCE MATERIEL COMMAND
KIRTLAND AIR FORCE BASE, NM 87117-5776

REPORT DOCUMENTATION PAGE

Form Approved
OMB No. 0704-0188

1. REPORT DATE *(DD-MM-YYYY)*	2. REPORT TYPE	3. DATES COVERED *(From - To)*
11-11- 2012	Journal Article	1 Mar 2012-1 Nov 2012

4. TITLE AND SUBTITLE

All Cavity-Magnetron Axial Extraction Technique (POSTPRINT)

5a. CONTRACT NUMBER
In-House

5b. GRANT NUMBER

5c. PROGRAM ELEMENT NUMBER

6. AUTHOR(S)

Brad W. Hoff, Andrew D. Greenwood, Michael D. Haworth, Peter J. Mardahl

5d. PROJECT NUMBER

5e. TASK NUMBER

5f. WORK UNIT NUMBER
D01K

7. PERFORMING ORGANIZATION NAME(S) AND ADDRESS(ES)
Air Force Research Laboratory
3550 Aberdeen Avenue SE
Kirtland AFB, NM 87117-5776

8. PERFORMING ORGANIZATION REPORT NUMBER

9. SPONSORING / MONITORING AGENCY NAME(S) AND ADDRESS(ES)

Air Force Research Laboratory
3550 Aberdeen Avenue SE
Kirtland AFB, NM 87117-5776

10. SPONSOR/MONITOR'S ACRONYM(S)
AFRL/RDHP

11. SPONSOR/MONITOR'S REPORT NUMBER(S)
AFRL-RD-PS-JA-2015-0001

12. DISTRIBUTION / AVAILABILITY STATEMENT
Approved for public release; distribution unlimited. 377ABW-2012-0362. Government Purpose Rights

13. SUPPLEMENTARY NOTES
Cleared 27 March 2012
Published to IEEE Transaction on Plasma Science; 11 November 2012

14. ABSTRACT
A compact axial π-mode extraction scheme, which is based on a patent by Greenwood, is demonstrated in conjunction with the UM/L-3 relativistic magnetron using the particle-in-cell code ICEPIC. Cases utilizing Greenwood's extraction technique were compared with power extraction using traditional radial waveguides. Average extracted power values in all simulated axial cases were found to be within +/−6.5% of the radial cases. Cases utilizing 85 degree and 90 degree sector waveguides were found to have efficiencies up to ten percentage points higher than the radial case. The best performing case was found to use a set of three axially oriented 90 degree sector waveguides, shorted on the upstream side, with the short located 15 cm from the center of the magnetron apertures.

15. SUBJECT TERMS
High power microwaves, relativistic magnetron, radio-frequency extraction

16. SECURITY CLASSIFICATION OF:			17. LIMITATION OF ABSTRACT	18. NUMBER OF PAGES	19a. NAME OF RESPONSIBLE PERSON
a. REPORT	b. ABSTRACT	c. THIS PAGE			Brad Hoff
UNCLASS	UNCLASS	UNCLASS	SAR	9	19b. TELEPHONE NUMBER *(include area*

Standard Form 298 (Rev. 8-98)
Prescribed by ANSI Std. 239.18

All Cavity-Magnetron Axial Extraction Technique

Brad W. Hoff, *Member, IEEE*, Andrew D. Greenwood, *Senior Member, IEEE*,
Peter J. Mardahl, and Michael D. Haworth

***Abstract*—A compact axial π-mode extraction scheme, which is based on a patent by Greenwood, is demonstrated in conjunction with the UM/L-3 relativistic magnetron using the particle-in-cell code ICEPIC. Cases utilizing Greenwood's extraction technique were compared with power extraction using traditional radial waveguides. Average extracted power values in all simulated axial cases were found to be within $+/-6.5\%$ of the radial cases. Cases utilizing 85° and 90° sector waveguides were found to have efficiencies up to ten percentage points higher than the radial case. The best performing case was found to use a set of three axially oriented 90° sector waveguides, shorted on the upstream side, with the short located 15 cm from the center of the magnetron apertures.**

***Index Terms*—High power microwaves, relativistic magnetron, radio-frequency extraction.**

I. Introduction

ARISING from efforts to develop compact relativistic magnetron-based sources, it was determined that traditional radial extraction designs, an example of which is shown in Fig. 1, did not conform to desired size constraints. Thus, a need to design a new way for extracting microwave power from a magnetron while maintaining a compact efficient package was developed. One technology of current interest, which potentially addresses this need, is the magnetron with diffractive output [1]–[3]. Another method, proposed by Greenwood [4], couples power into an array of axially oriented sector waveguides. Greenwood's extraction method is the focus of the computational studies presented here.

II. Background

Greenwood's extractor design was derived from considering the magnetic coupling employed by a rectangular slotted waveguide antenna and applying reciprocity. A piece of a typical slotted waveguide antenna, designed to radiate the lowest order (TE_{10}) mode, is shown in Fig. 2. Note that, in order to radiate, the slots must be placed such that the current on the waveguide wall is interrupted. For a TE_{10} mode propagating in

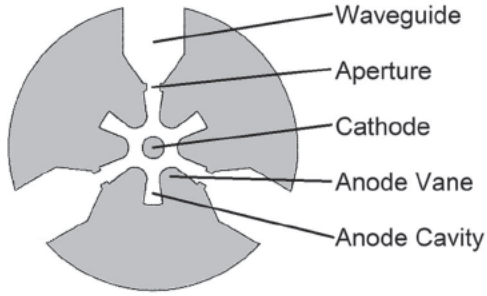

Fig. 1. Depiction of a relativistic magnetron using a radial extraction scheme.

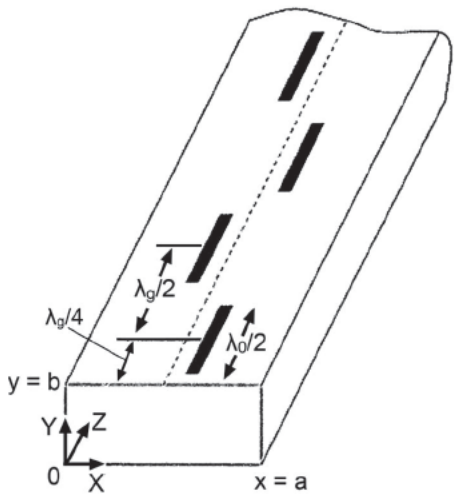

Fig. 2. Slotted waveguide shorted at $z = 0$.

a hollow waveguide, the time harmonic electromagnetic fields in phasor form ($e^{-i\omega t}$ time convention) are given by

$$E = \hat{y} E_0 \sin\left(\frac{\pi}{a}x\right) e^{ik_z z} \tag{1}$$

$$H = \frac{E_0}{\eta_0}\left[-\hat{x}\frac{k_Z}{k}\sin\left(\frac{\pi}{a}x\right) - \hat{z}i\frac{\pi}{ka}\cos\left(\frac{\pi}{a}x\right)\right] e^{ik_z z} \tag{2}$$

where e_0 is the wave amplitude, η_0 is the impedance of free space, $k = \omega/c = 2\pi/\lambda 0$ is the free-space electromagnetic wavenumber, ω is the radial frequency, c is the speed of light, $k_z = [k^2 - (\pi/a)^2]^{0.5} = 2\pi/\lambda_g$ is the waveguide propagation constant, λ_0 is the free-space electromagnetic wavelength, λ_g is the guided wavelength, and $i = (-1)^{0.5}$. The surface current density in the top waveguide wall is then given by

$$J_s = -\hat{y} \times H$$
$$= \frac{E_0}{\eta_0}\left[\hat{x}i\frac{\pi}{ka}\cos\left(\frac{\pi}{a}x\right) - \hat{z}\frac{k_z}{k}\sin\left(\frac{\pi}{a}x\right)\right] e^{ik_z z}. \tag{3}$$

Manuscript received March 26, 2012; revised June 11, 2012, July 9, 2012, and August 1, 2012; accepted August 30, 2012. Date of publication October 3, 2012; date of current version November 6, 2012. This work was supported in part by the Air Force Research Laboratory, by the Air Force Office of Scientific Research under Grant AFOSR LRIR 11RD01COR, and by the Department of Defense High Performance Computer Modernization Program under Subproject AFKED01314C4O.

The authors are with the Directed Energy Directorate, Air Force Research Laboratory, Kirtland Air Force Base, Albuquerque, NM 87117 USA.

Color versions of one or more of the figures in this paper are available online at http://ieeexplore.ieee.org.

Digital Object Identifier 10.1109/TPS.2012.2217758

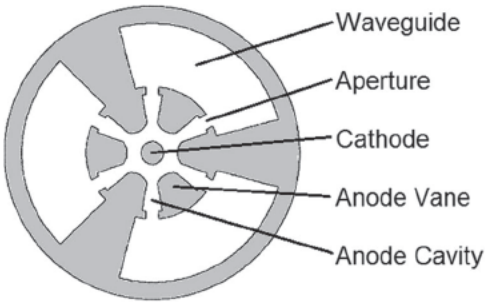

Fig. 3. Depiction of a relativistic magnetron cross section using Greenwood's extraction concept.

Thus, the transverse (x-directed) current on the top wall has a cosine distribution with a null value along the center axis of the wall. A slot cut along the center axis of the wall does not radiate, which is the reason that the slots in Fig. 2 are located off the center axis. Furthermore, the radiation from two side-by-side slots, symmetric about the center axis of the wall, is 180° out of phase and tends to cancel. Thus, the slots on the opposite sides of the center axis of the wall are spaced by one-half of a waveguide wavelength ($\lambda_g/2$); therefore, the radiation is in phase. By reciprocity, to excite a TE_{10} mode in a rectangular waveguide through a slot in the broad wall of the waveguide, the slot must be located off the center axis of the wall. Two side-by-side slots on opposite sides of the center axis excite the TE_{10} mode if they are driven 180° out of phase.

Conventional and relativistic magnetrons are, in general, preferentially operated in the π mode [5]–[7], which is characterized by a phase shift of π rad (180°) between the fields in adjacent cavities. Thus, based on the preceding discussion, a set of two adjacent cavities could be used to drive the fundamental mode in a single waveguide.

Due to the constraints of the cylindrical geometry of the relativistic magnetron, in order to connect the two adjacent magnetron cavities, a double-baffled cylindrical coaxial sector waveguide is used instead of a rectangular one. It is important to note that differences exist between the sector waveguide fundamental mode (TE_{11}) and the rectangular waveguide fundamental mode (TE_{10}), due to the curvature of the sector waveguides; however, the aforementioned general method of coupling electromagnetic energy into and out of the waveguides will still apply. The coupling of electromagnetic energy into the sector waveguide TE_{11} mode will be further treated in the following sections. Fig. 3 depicts an example of a six-vane relativistic magnetron coupled to a set of three 90° sector waveguides.

III. ICEPIC Simulations

The University of Michigan's UM/L-3 relativistic magnetron, which has previously been studied both computationally and experimentally [8]–[13], was chosen to be the test case used to compare Greenwood's extraction technique against traditional radial extraction methods. Simulations comparing the two extraction methods were carried out using ICEPIC [14].

Fig. 4 shows cross-sectional geometry for the UM/L-3 relativistic magnetron in the radial extraction configuration

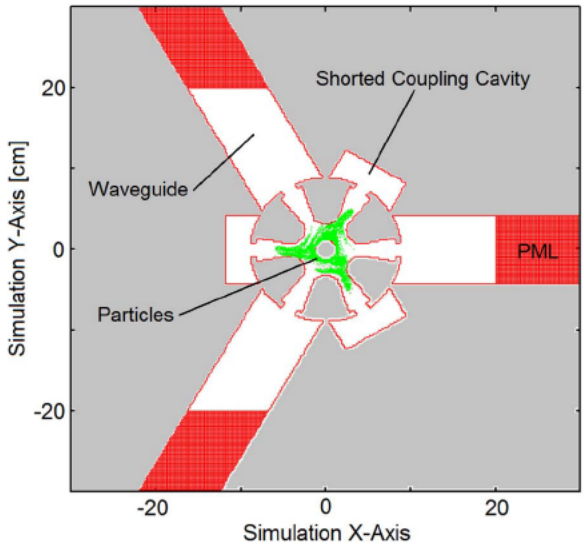

Fig. 4. Simulation geometry for the radially extracted case. Particle configurations shown are for π-mode operation at $B_z = 0.25$ T at 400 ns.

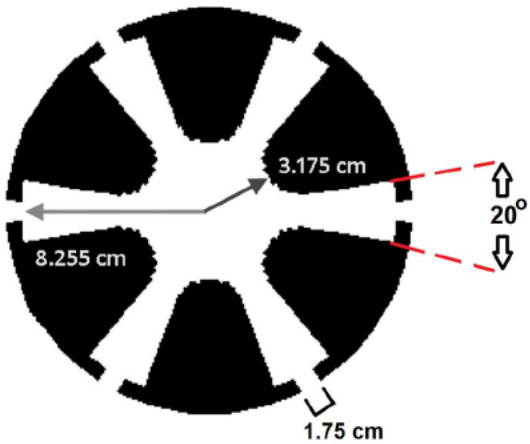

Fig. 5. Physical geometry of the UM/L-3 relativistic magnetron anode. Features are resolved to within the 2 mm × 2 mm × 2 mm Cartesian grid utilized in the ICEPIC simulations.

used in the radially extracted control case. This is the same extraction method used in previously published work [8]–[13]. Radial waveguides are connected to every other coupling cavity, whereas the remaining cavities are shorted with metal plates. Waveguide loads were implemented using the perfectly matched layer (PML) boundary condition [15], [16]. The simulation geometry for the radial case is the same as that used in [13], with the exception of the larger 2.5-cm-diameter cathode used here. Additional details on the UM/L-3 relativistic magnetron anode block are provided in Fig. 5. Electrostatic end balls were included on both the upstream and downstream portions of the cathode to reduce end-loss current from the magnetron. A Cartesian grid was utilized in all simulations. Grid resolution along all three axes for all simulations performed was 2 mm.

An example of simulation geometry initialized in the cases using Greenwood's extraction method is shown in Fig. 6. In the first set of simulations, each of the three sector waveguides

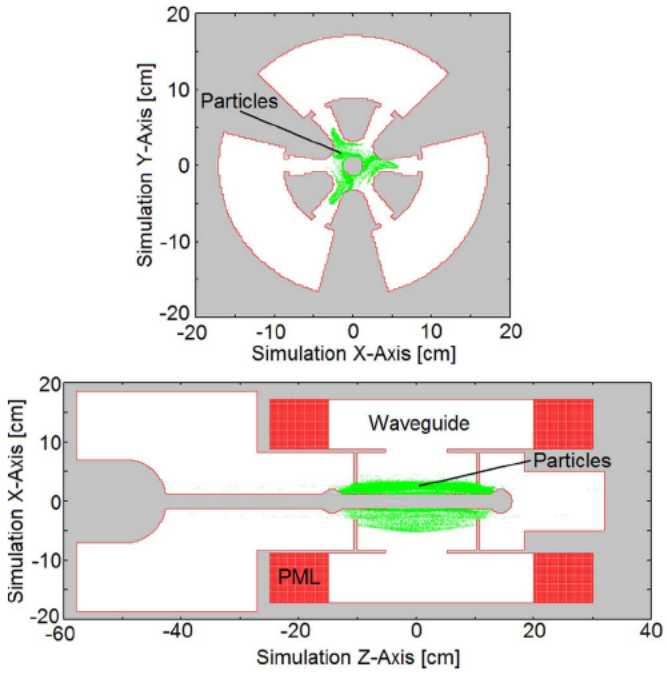

Fig. 6. Simulation geometry for the axially extracted case using 90° sector waveguides. Particle configurations shown are for π-mode operation at $B_z = 0.25$ T at 400 ns.

was terminated at both ends using a PML. The radial height of each of the sector waveguides was 8.25 cm. Extraction cases using waveguide sector angles of 85°, 90°, 95°, and 100° were simulated. Each of the sector waveguides had an inner radius of approximately 8.9 cm and an outer radius of 17.1 cm. Cutoff frequencies for each of the waveguides, calculated as per [17] and [18] for the lowest order mode (TE_{11}), were found to be 781, 738, 700, and 665 MHz for the of 85°, 90°, 95°, and 100° sector waveguides, respectively.

Cold test simulations were performed on the radially extracted case and all four axially extracted cases. The cold π-mode frequency of the radial case was found to be 1.035 GHz. The cold π-mode frequency was reduced to 1.030 GHz in the 85° sector angle case and was found to drop by 20 MHz for every additional 5° of angular width up through 100°.

Fig. 7(a) depicts power, voltage, current, and efficiency data from the radial extraction in which the applied magnetic field was 0.25 T. A fast Fourier transform of the voltage across one of the magnetron cavities is shown in Fig. 7(b). Simulations for both the radial extraction cases and the axial extraction cases were performed using magnetic fields ranging from 0.25 to 0.30 T. In all simulations, the unloaded (zero current emission) voltage across the 2-cm anode–cathode (A–K) gap was set to 300 kV. Due to the constant impedance of the voltage input boundary, as net current drawn by the magnetron increased, the A–K gap voltage drooped linearly. Fig. 8 depicts a plot of net cathode current drawn by the magnetron versus the A–K gap voltage during steady-state operation for all extraction cases at magnetic fields within the previously stated range.

Steady-state extracted power as a function of applied magnetic field for all extraction cases is plotted in Fig. 9(a). Fig. 9(b) displays the corresponding operating efficiencies for each magnetic field case. All axial extraction cases examined were found

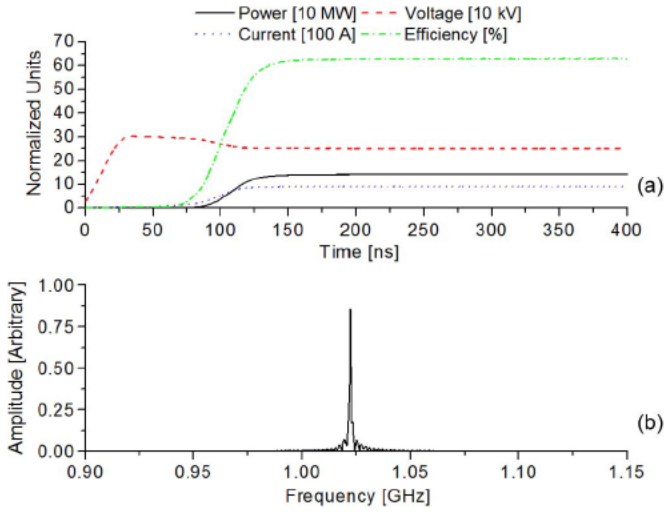

Fig. 7. (a) Power, voltage, current, efficiency, and (b) operating frequency for the radially extracted case at $B_z = 0.25$ T.

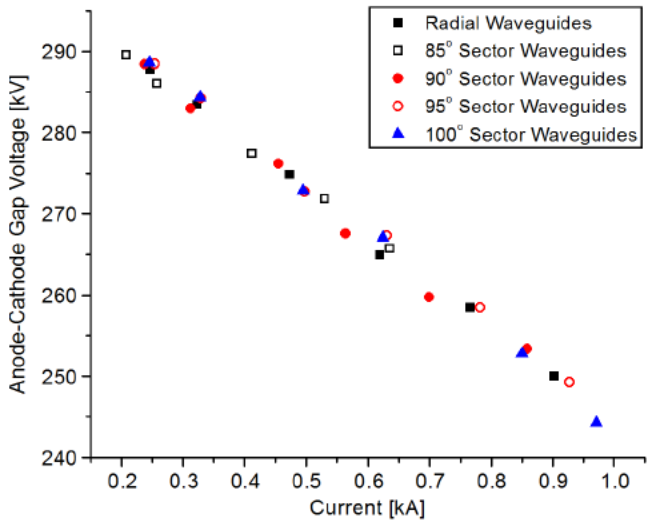

Fig. 8. A–K gap voltage as a function of net cathode current drawn at steady-state magnetron operation.

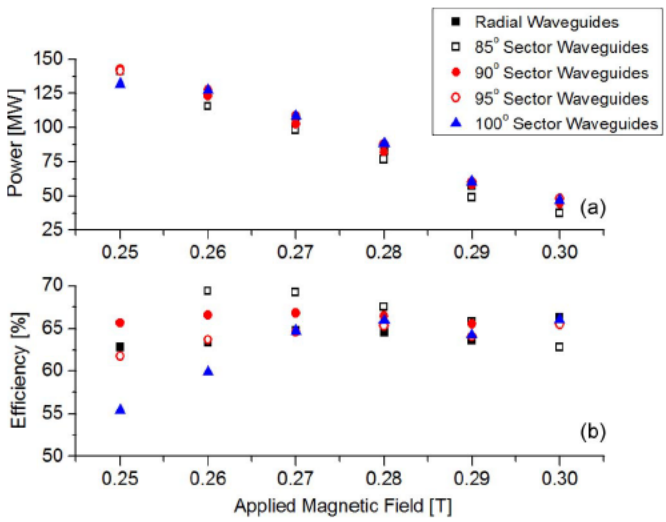

Fig. 9. (a) Power as a function of applied magnetic field and (b) efficiency as a function of applied magnetic field for all extraction cases.

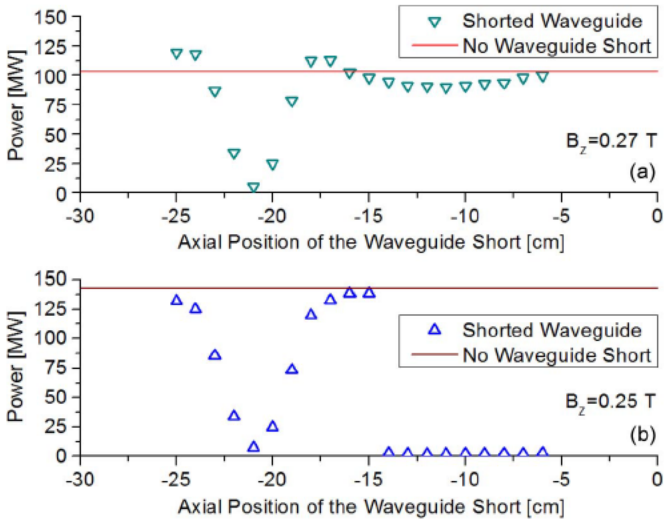

Fig. 10. Extracted power as a function of waveguide short location for (a) the $B_z = 0.27$ T case and (b) the $B_z = 0.25$ T case. For comparison, total extracted power for each magnetic field case utilizing unshorted waveguides is also indicated.

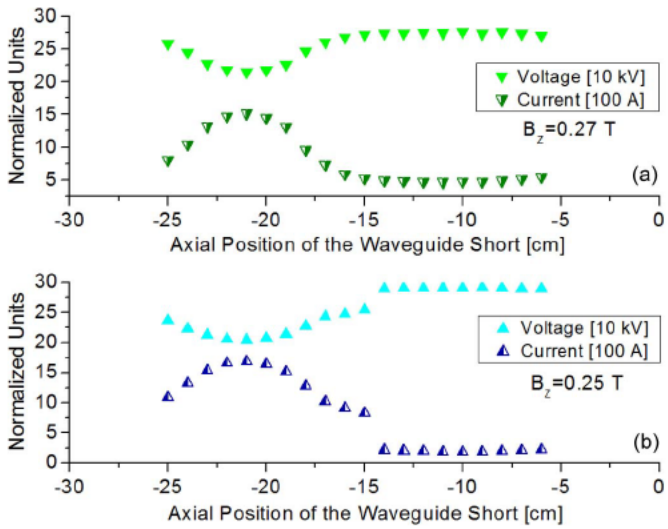

Fig. 11. Steady-state voltage and current as a function of waveguide short location for (a) the $B_z = 0.27$ T case and (b) the $B_z = 0.25$ T case.

to have output power values within $+/-10$ MW of the radial extraction case. The 85° and 90° sector waveguide cases did exhibit higher efficiency than the radial extraction cases at all but the highest magnetic field values. As previously mentioned, cathode end loss current was suppressed in all simulations due to the inclusion of nonemitting electrostatic end balls on the cathode. Enhanced end loss current would reduce magnetron efficiencies to values closer to those described in previous work [8]–[13].

Because the 90° sector waveguide case showed the best balance of power and efficiency, it was chosen as the study case for inclusion of waveguide shorts on the upstream side of the waveguides. Fig. 10 depicts data from two magnetic field cases in which a range of axial positions for the waveguide short were simulated. Length values given are the magnitude of the distance between the axial center of the 10.6-cm-long magnetron apertures and the z-coordinate of the waveguide short. Steady-state voltage and current data corresponding to the simulation data presented in Fig. 10 are provided in Fig. 11.

At a frequency of 1.025 GHz, the guided wavelength for the fundamental mode of the 90° sector waveguides was calculated to be 42.2 cm. Thus, for the maximum power transfer in the $+z$-direction, waveguide shorts should, theoretically, be placed a quarter wavelength away from the center of the magnetron apertures at approximately $z = -10.5$ cm. Placing the waveguide shorts at one-half wavelength from the center of the magnetron apertures ($z = -21.1$ cm) should result in the little or no power extraction in the $+z$ direction.

Interestingly, in the $B_z = 0.25$ T case, when the distance between the waveguide short and the center of the magnetron apertures ranged from 6 to 14 cm, the magnetron oscillated in an unextractable 1.754-GHz $2\pi/3$-like transverse mode with a higher order axial mode, as shown in Fig. 12, instead of the expected 1.025-GHz π mode. The $B_z = 0.27$ T case did not experience a noticeable mode shift for waveguide short locations in the same 6–14-cm range but did experience a nearly 25-MHz reduction in π-mode frequency in this range, suggesting the short locations were still interfering with π-mode operation, possibly through enhancement of the competing higher order mode observed in the $B_z = 0.25$ T case. Due to the presence of the competing high-order mode, the best waveguide short position was found to be at $z = -15$ cm.

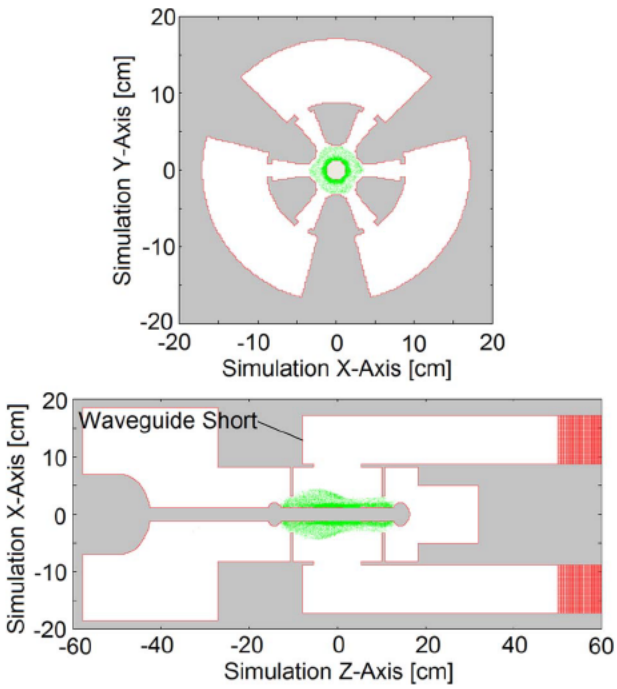

Fig. 12. Undesired axial mode observed in the 90° sector waveguide cases with $B_z = 0.25$ T and waveguide short locations in the range of 6 to 14 cm from the center of the magnetron apertures.

Simulation geometry and particle plots are shown in Fig. 13(a) and (b) for the xy plane and the xz plane of one of the 90° sector waveguide cases with $B_z = 0.25$ T and a waveguide short located 15 cm from the center of the magnetron apertures. In these figures, the magnetron is operating correctly in the π mode. Pseudocolor plots of the electric field for this same case are provided in Fig. 14(a) and (b).

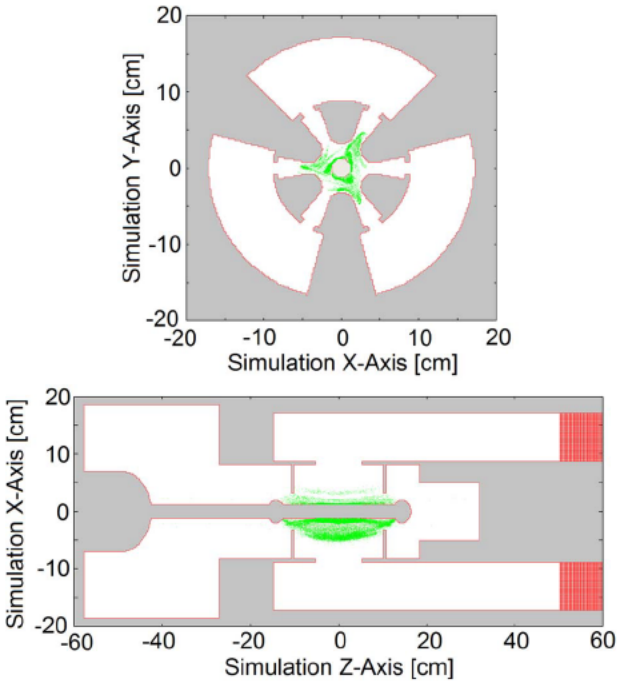

Fig. 13. (a) xy plane cross section and (b) xz plane cross section of the simulation magnetron operation in the π mode, using shorted 90° sector waveguide case with $B_z = 0.25$, with waveguide shorts located 15 cm from the center of the magnetron apertures.

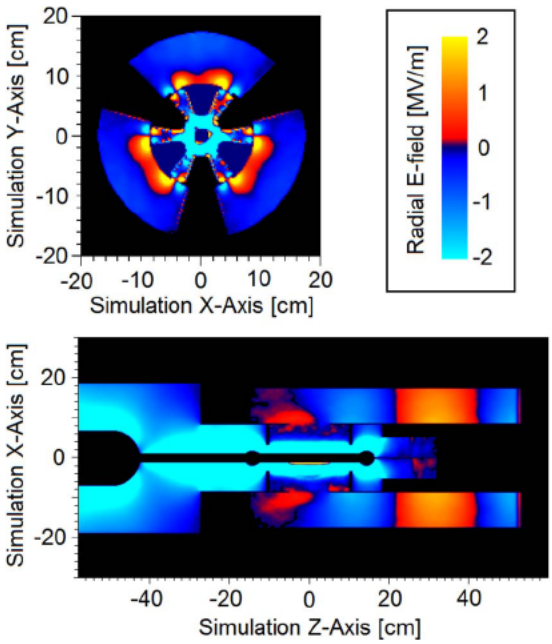

Fig. 14. Pseudocolor plot of the radial component of the electric field during π-mode operation of the 90° sector waveguide case with $B_z = 0.25$ with waveguide shorts located 15 cm from the center of the magnetron apertures.

IV. Summary and Conclusion

Simulations comparing Greenwood's axial extraction technique with traditional radial extraction methods were performed, using the UM/L-3 magnetron geometry. The initial set of simulations compared magnetron performance using radial extraction with using bidirectional axial extraction into sets of sector waveguides. In all cases tested, axially extracted power was within $+/-6.5\%$ of power extracted in the radial case. Overall, the axially extracted case using 90° sector waveguides was chosen as the best performing case due to equaling the radially extracted case in both power and slightly exceeding the radially extracted case in efficiency in for all magnetic field values used.

Subsequent simulations, focusing on the 90° sector waveguide case, implemented a waveguide short on all upstream $(-z)$ waveguides such that all power was extracted in the downstream $(+z)$ loads. Results from these simulations showed that, in addition to the expected waveguide interference patterns due to the position of the waveguide short, there were regions in which placement of the waveguide shorts negatively affected the operating mode of the magnetron. For example, at an axial magnetic field value of 0.25 T, when the waveguide shorts were located anywhere in the range of 6 to 14 cm from the center of the magnetron apertures, instead of operating in the expected π mode, the magnetron was forced into operating in a $2\pi/3$-like transverse mode with a higher order axial mode, which resulted in zero extracted power. In the cases simulated, locating the waveguide shorts 15 cm from the center of the magnetron apertures resulted in the best performance.

It is well known that the loading caused by radio-frequency extraction methods can have a strong effect on the operating mode of a magnetron [5]. Because the UM/L-3 anode geometry was originally designed for use with a radial extraction scheme, it is not entirely surprising that changing the extraction method would introduce unwanted mode competition. It is reasonable to expect that minor modifications to the anode and extraction apertures could be performed to help suppress the higher order mode and optimize magnetron performance with the axial extraction scheme.

References

[1] N. F. Kovalev, B. D. Kol'chugin, V. E. Nechaev, M. M. Ofitserov, E. I. Soluyanov, and M. I. Fuks, "Relativistic magnetron with diffraction output," *Sov. Tech. Phys. Lett.*, vol. 3, pp. 430–431, Oct. 1977.

[2] M. Daimon and W. Jiang, "Modified configuration of relativistic magnetron with diffraction output for efficiency improvement," *Appl. Phys. Lett.*, vol. 91, no. 19, pp. 191503-1–191503-3, Nov. 2007.

[3] M. I. Fuks and E. Schamiloglu, "70% efficient relativistic magnetron with axial extraction of radiation through a horn antenna," *IEEE Trans. Plasma Sci.*, vol. 38, no. 6, pp. 1302–1312, Jun. 2010.

[4] A. D. Greenwood, "All cavity magnetron axial extractor," U.S. Patent 7 106 004, Sep. 12, 2006.

[5] G. B. Collins, Ed., *Microwave Magnetrons*, 1st ed. New York: McGraw-Hill, 1948.

[6] A. Palevsky and G. Bekefi, "Microwave emission from pulsed, relativistic E-beam diodes. II. The multiresonator magnetron," *Phys. Fluids*, vol. 22, no. 5, pp. 986–996, May 1979.

[7] J. Benford, J. A. Swegle, and E. Schamiloglu, *High Power Microwaves*, 2nd ed. London, U.K.: Taylor & Francis, 2007.

[8] M. R. Lopez, R. M. Gilgenbach, M. C. Jones, W. M. White, D. W. Jordan, M. D. Johnston, T. S. Strickler, V. B. Neculaes, Y. Y. Lau, T. A. Spencer, M. D. Haworth, K. L. Cartwright, P. J. Mardahl, J. W. Luginsland, and D. Price, "Relativistic magnetron driven by a microsecond E-beam accelerator with a ceramic insulator," *IEEE Trans. Plasma Sci.*, vol. 32, no. 3, pp. 1171–1180, Jun. 2004.

[9] P. Mardahl, K. Cartwright, A. Greenwood, M. Haworth, L. Bowers, T. Murphy, T. Spencer, R. Gilgenbach, M. Lopez, J. Watrous, and J. Luginsland, "Numerical model of the MELBA-C relativistic magnetron using 3D PIC," in *Proc. Amer. Phys. Soc. 45th Annu. Meet. Division Plasma Phys.*, Albuquerque, NM, 2003.

[10] M. C. Jones, V. B. Neculaes, R. M. Gilgenbach, W. M. White, M. R. Lopez, Y. Y. Lau, T. A. Spencer, and D. Price, "Projection ablation

lithography cathode for high-current, relativistic magnetron," *Rev. Sci. Instrum.*, vol. 75, no. 9, pp. 2976–2980, Sep. 2004.

[11] J. T. Fleming, P. Mardahl, L. Bowers, H. Bosman, S. Prasad, M. Fuks, and E. Schamiloglu, "Three dimensional PIC simulations of the transparent and eggbeater cathodes in the Michigan relativistic," in *Proc. 33rd IEEE Int. Conf. Plasma Sci.*, 2006, p. 338.

[12] B. W. Hoff, R. M. Gilgenbach, N. M. Jordan, Y. Y. Lau, E. J. Cruz, D. M. French, M. R. Gomez, J. C. Zier, T. A. Spencer, and D. Price, "Magnetic priming at the cathode of a relativistic magnetron," *IEEE Trans. Plasma Sci.* , vol. 36, no. 3, pp. 710–717, Jun. 2008.

[13] B. W. Hoff, P. J. Mardahl, R. M. Gilgenbach, M. D. Haworth, D. M. French, Y. Y. Lau, and M. Franzi, "Microwave window breakdown experiments and simulations on the UM/L-3 relativistic magnetron," *Rev. Sci. Instrum.*, vol. 80, no. 9, pp. 094702-1–094702-9, Sep. 2009.

[14] R. E. Peterkin and J. W. Luginsland, "A virtual prototyping environment for directed-energy concepts," *Comput. Sci. Eng.*, vol. 4, no. 2, pp. 42–49, Mar./Apr. 2002.

[15] B. Jean-Pierre, "A perfectly matched layer for the absorption of electromagnetic waves," *J. Comput. Phys.*, vol. 114, no. 2, pp. 185–200, Oct. 1994.

[16] D. S. Katz, E. T. Thiele, and A. Taflove, "Validation and extension to three dimensions of the Berenger PML absorbing boundary condition for FD-TD meshes," *IEEE Microw. Guided Wave Lett.*, vol. 4, no. 8, pp. 268–270, Aug. 1994.

[17] S. Flugge, Ed., "Electromagnetic waveguides and resonators," in *Encyclopedia of Physics*. Berlin, Germany: Springer-Verlag, 1958, p. 345.

[18] C. C. Courtney and D. E. Voss, "Modes of a double-baffled, cylindrical, coaxial waveguide," in *Voss Scientific, LLC*, Albuquerque, NM, Aug. 2003, pp. 1–18.

Brad W. Hoff (S'04–M'10) received the B.S. degree in physics from the U.S. Naval Academy, Annapolis, MD, in 1999 and the M.S.E. degree in nuclear engineering, the M.S.E. degree in electrical engineering, and the Ph.D. degree in nuclear engineering from the University of Michigan, Ann Arbor, in 2006, 2007, and 2009, respectively.

He is currently a Research Physicist with the Directed Energy Directorate, Air Force Research Laboratory, Kirtland Air Force Base, Albuquerque, NM. His research interests include high-power microwave sources and directed energy technology.

Andrew D. Greenwood (SM'06) received the B.S. and M.S. degrees in electrical engineering from Brigham Young University, Provo, UT, in 1993 and 1995, respectively, and the Ph.D. degree in electrical engineering from the University of Illinois at Urbana-Champaign, Urbana, in 1998, where he studied the use of the finite-element method to compute electromagnetic scattering and radiation from axisymmetric bodies.

In 1996, he joined the Rome Laboratory as a Palace Knight employee, and in 1998, he joined the Directed Energy Directorate, Air Force Research Laboratory, Kirtland Air Force Base, Albuquerque, NM, where he conducts research on particle-in-cell methods to simulate high-power microwave devices.

Peter J. Mardahl received the two B.S. degrees in electrical engineering and nuclear engineering and the Ph.D. degree in electrical engineering from the University of California, Berkeley, Berkeley, in 1992 and 2001, respectively.

In 2002, he joined the Air Force Research Laboratory, Kirtland Air Force Base, Albuquerque, NM. He is now working as a Computational Physicist studying high-power microwave devices. His research interests include simulated laser–plasma interactions, high-power magnetron design, and particle-in-cell code development.

Michael D. Haworth received the B.S. degree in physics and the M.S. and Ph.D. degrees in plasma physics from Auburn University, Auburn, AL, in 1977, 1978, and 1983, respectively.

He is currently working with the Directed Energy Directorate, Air Force Research Laboratory, Kirtland Air Force Base, Albuquerque, NM. His primary research interests include relativistic magnetrons.

DISTRIBUTION LIST

DTIC/OCP
8725 John J. Kingman Rd, Suite 0944
Ft Belvoir, VA 22060-6218 1 cy

AFRL/RVIL
Kirtland AFB, NM 87117-5776 1 cy

Official Record Copy
AFRL/RDHP/Brad Hoff 1 cy